

## Powder Metallurgy HIP and Extrusion Study of FeCrAl Alloy for Accident Tolerant Fuel Cladding

Shenyan Huang<sup>1,a\*</sup>, Evan Dolley<sup>1,b</sup>, Steve Buresh<sup>1,c</sup>, Ian Spinelli<sup>1,d</sup>,  
Jason Leszczewicz<sup>1,e</sup>, Marija Drobnjak<sup>1,f</sup>, Mike Knussman<sup>1,g</sup>, Raul B. Rebak<sup>1,h</sup>

<sup>1</sup>GE Research, 1 Research Circle, Niskayuna NY, 12309, USA

<sup>a</sup>huangs@ge.com, <sup>b</sup>dolley@ge.com, <sup>c</sup>buresh@ge.com, <sup>d</sup>spinelli@ge.com,

<sup>e</sup>Jason.Leszczewicz@ge.com, <sup>f</sup>marija.drobnjak@ge.com, <sup>g</sup>knussman@ge.com, <sup>h</sup>rebak@ge.com

**Keywords:** FeCrAl, Accident Tolerant Fuel, Nuclear Materials, Powder Metallurgy, HIP

**Abstract.** Powder metallurgy HIP and extrusion processing conditions were investigated in a FeCrAl alloy (Fe-Cr-Al-Mo based PM-C26M) for accident tolerant fuel cladding applications. The powder size range, HIP temperature (900 ~ 1100°C), HIP time (2 hours vs. 4 hours) were varied in lab-scale experiments, using argon gas atomized powder. The resulting density, grain size distribution, and retained plastic strain were characterized to recommend the HIP condition with full consolidation, fine grain size for formability, and good powder economics. The subsequent extrusion process was also studied in the temperature range of 950 ~ 1050°C as well as post annealing conditions. Based on the microstructure evaluation, sensitivity of HIP and extrusion process parameters were better understood.

### Introduction

During the last decade, the international nuclear materials community was studying the possibility of replacing the zirconium based nuclear fuel cladding with materials that would be more tolerant of a loss-of-coolant accident. One of the most promising alternatives is to use tubes of FeCrAl alloys for the cladding of the fuel [1-3]. FeCrAl alloys have extraordinary resistance to attack by superheated steam and offer good mechanical and corrosion resistance properties under light water reactors normal operation conditions [4,5]. FeCrAl alloys were studied extensively in the 1960s for nuclear materials applications [2]. Even then it was recognized that the traditional alloy fabrication process of melting, casting, and forging was not the most promising for this family of alloys. The powder metallurgy process was more efficient since it resulted in reliable quality extruded bar stock that can be later pilgered into 5 m long 10 mm diameter tubes with a wall thickness down to 0.3 mm [4]. The objective of this work was to understand the processing window and sensitivity of HIP and extrusion parameters for the newer PM-C26M FeCrAl alloy, which does not have oxide dispersion strengthening nano particles that are characteristics of the more traditional APMT alloy.

### Influence of HIP temperature, time, powder size range

Argon gas atomized PM-C26M powder was obtained from Sandvik with the actual composition of Fe-12.2Cr-5.7Al-2Mo in weight percent. As-received powder had a size range of 20 ~ 500 µm and tap density of 4.56 g/cm<sup>3</sup> (or relative tap density 64%). D10, D50, D90 of as-received powder were 44.6, 103.0, 206.6 µm, respectively. A representative powder morphology and cross-section microstructure is shown in Fig. 1. Powder particles are mostly spherical with some satellites and trapped round argon pores inside powder, revealing equiaxed grain structure regardless of individual powder particle size. Two powder size ranges were studied for HIP processing, including the as-received 20 ~ 500 µm and the 20 ~ 250 µm (coarse particles sieved out). Subscale cylindrical HIP canisters of 19 mm diameter and 51 mm height were filled with powder, outgassed, helium leak checked, and then HIP'ed to get full powder densification. Detailed parameters are



summarized in Table 1. All of the HIP cycles were performed with a simultaneous linear ramp of temperature (10°C/min) and pressure followed by a furnace cool after the HIP cycle in the Moly 5.5 inch Moly HIP unit at American Isostatic Presses. Two canisters with different powder size ranges and the same HIP parameters were HIP processed in the same cycle, to prevent process variation or introduction of a lurking variable. Ten HIP cycles were performed for the study.

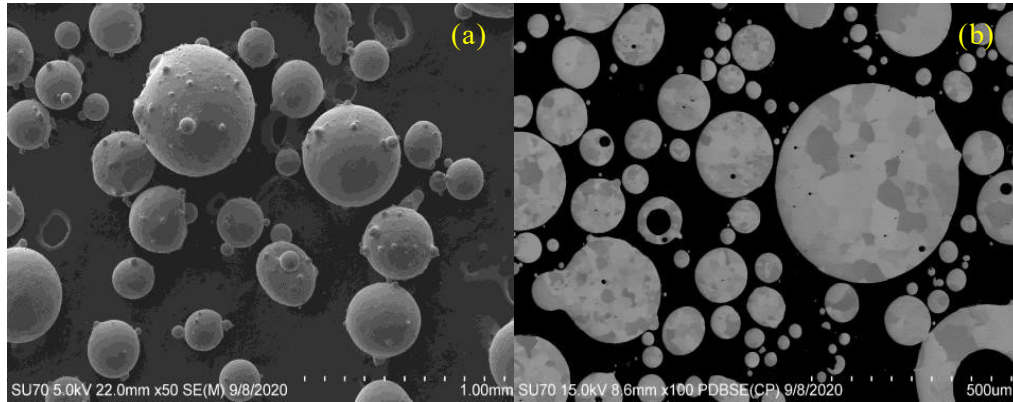


Figure 1: (a) Secondary electron image of as-received PM-C26M argon gas atomized powder particles; (b) backscattered electron image of powder cross sections.

Table 1: Detailed powder size range and HIP parameters in the HIP study. The average grain size measured by EBSD is specified for select conditions.

	900°C 15ksi 2hr	900°C 15ksi 4hr	950°C 15ksi 2hr	950°C 15ksi 4hr	980°C 15ksi 2hr	980°C 15ksi 4hr	1050°C 15ksi 2hr	1050°C 15ksi 4hr	1100°C 15ksi 2hr	1100°C 15ksi 4hr
20~250µm	X	X	--	--	X	X, 20µm	X	X, 21µm	X	X, 26µm
20~500µm	X	X	X	X, 18µm	X	X, 20µm	X	X, 28µm	X	X, 35µm

After HIP, the canisters were machined to remove canister material. The obtained cylinders of the consolidated PM-C26M were measured for density using the Archimedes method. Fig. 2(a) plots the resulting densities as a function of HIP temperature, time, and powder size range. It clearly shows that HIP temperature higher than 980°C achieved full density. HIP time of 2 hours seems sufficient for the lab-scale small HIP cans, as longer HIP time of 4 hours didn't result in a density increase. A similar trend is observed for the two powder size ranges studied. A minimum of 3 hours HIP time may be required for larger HIP cans, considering additional time needed for equilibrium temperature/pressure. Lower HIP temperatures of 900°C and 950°C failed to achieve full densification, even at 4 hours of HIP time. An example of 900°C HIP microstructure is displayed in Fig. 2(b), indicating residual porosity inside the prior powder particles or at the powder particle boundaries. Porosity inside the prior powder particles are likely the trapped argon gas porosities originated from the gas atomization process that were not fully closed by the HIP cycles due to insufficient temperature for the diffusional process.

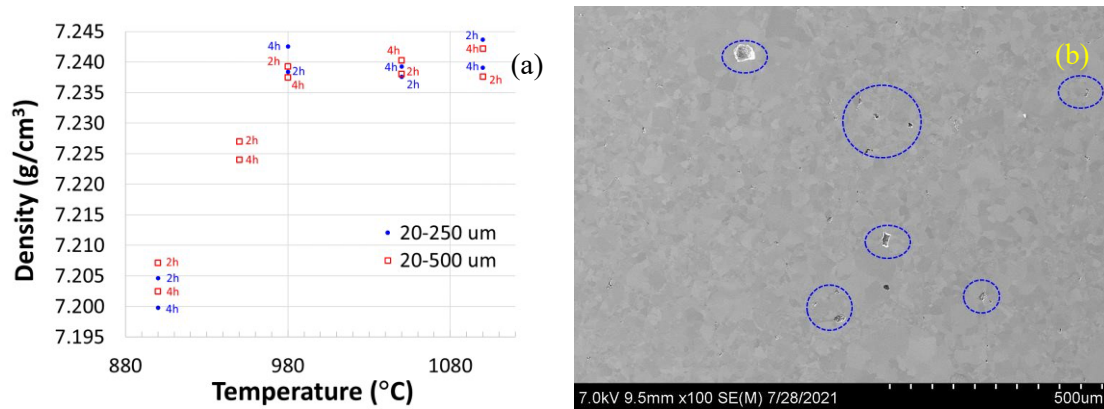


Figure 2: (a) Post-HIP density of PM-C26M as a function of HIP temperature, time, powder size range; (b) secondary electron image of the resulting microstructure with 900°C/15ksi/4hr HIP condition and 20~250 μm powder size range. Blue circles highlight the residual porosity.

The resulting grain structures as a function of HIP temperature and powder size range are presented in Fig. 3, with HIP temperature from high to low and two powder size ranges side by side for the same HIP condition. It is observed that the 20 ~ 500 μm powder size range with higher fraction of coarse powder particles generates severe grain growth in the larger powder particles (>200 μm) at higher HIP temperatures of 1050 and 1100°C. As a result, some coarse powder particles even became single grain, since there were few secondary precipitates in PM-CM26 to effectively pin grain boundary migration and thermal energy at 1050 and 1100°C HIP temperatures dominated grain growth. In comparison, the level of grain growth in the 20 ~ 250 μm powder size range was less severe due to lack of large powder particles above 250 μm. These large grains or single-grain powder particles could add difficulty to the processability of the subsequent bar extrusion. When HIP temperature was reduced to 980°C, finer grain structure absent of single grain powder particles was observed, which appeared to be adequate as-HIP grain structure for the subsequent extrusion. 980°C HIP didn't reveal a large sensitivity with respect to the powder size range. Although 900°C HIP shows an even finer grain size, the residual porosities from partial consolidation could cause crack initiation in extrusion and thus was not further considered.

Detailed EBSD characterization was performed on the select conditions to quantify the grain size distribution, average grain size, and evaluate the retained plastic strain. Hitachi SU-70 FEGSEM with Oxford Aztec Symmetry EBSD was used. A 20kV accelerating voltage, 0.25 μm step size, 1000 x 750 μm scan area were applied. Additional maps were acquired for 1050 and 1100°C HIP with a 20 ~ 500 μm powder size range to ensure good statistical representation of the coarse grains. The total grain count for each condition was in the range of 2000 ~ 5000. Average grain size was quantified by line intercept method and the calculated mean intercept length is specified in Table 1, which verified the fine grain size (20 μm) in 980°C HIP and the grain growth (up to 35 μm average grain size) in the coarse powder size at higher HIP temperatures. The cumulative frequency of grain size plot and grain size distribution plots in Fig. 4 further indicate the grain size shifting to the large size and wider distribution with higher HIP temperature and coarser powder. Kernel average misorientation maps were also acquired to qualitatively reveal the retained plastic strain (not shown herein due to space limitations). In general, the retained plastic strain for the characterized conditions was quite low. Grain boundary maps for HIP temperatures at or above 980°C suggest ~20% of low angle boundaries (3 ~ 10°) and Σ3 special boundaries in the HIP conditions and largely recrystallized structure. While the 950°C HIP condition shows ~25% low angle boundaries localized at the space between powder particles.

The measured average Vickers microhardness for all the studied conditions was in the range of 211 ~ 221 HV. There was no obvious hardness difference in various conditions given the standard deviation. One additional drawback of having coarse powder particles was found to be the coarse powder particles transporting to the upper portion of HIP can during vibrational powder packing step before outgassing step. Coarse powder particle separation is a concern for large HIP parts. Therefore, the most reasonable condition found in the study seems to be 20 ~ 250  $\mu\text{m}$  powder size range and 980°C/15ksi/4hr HIP condition.

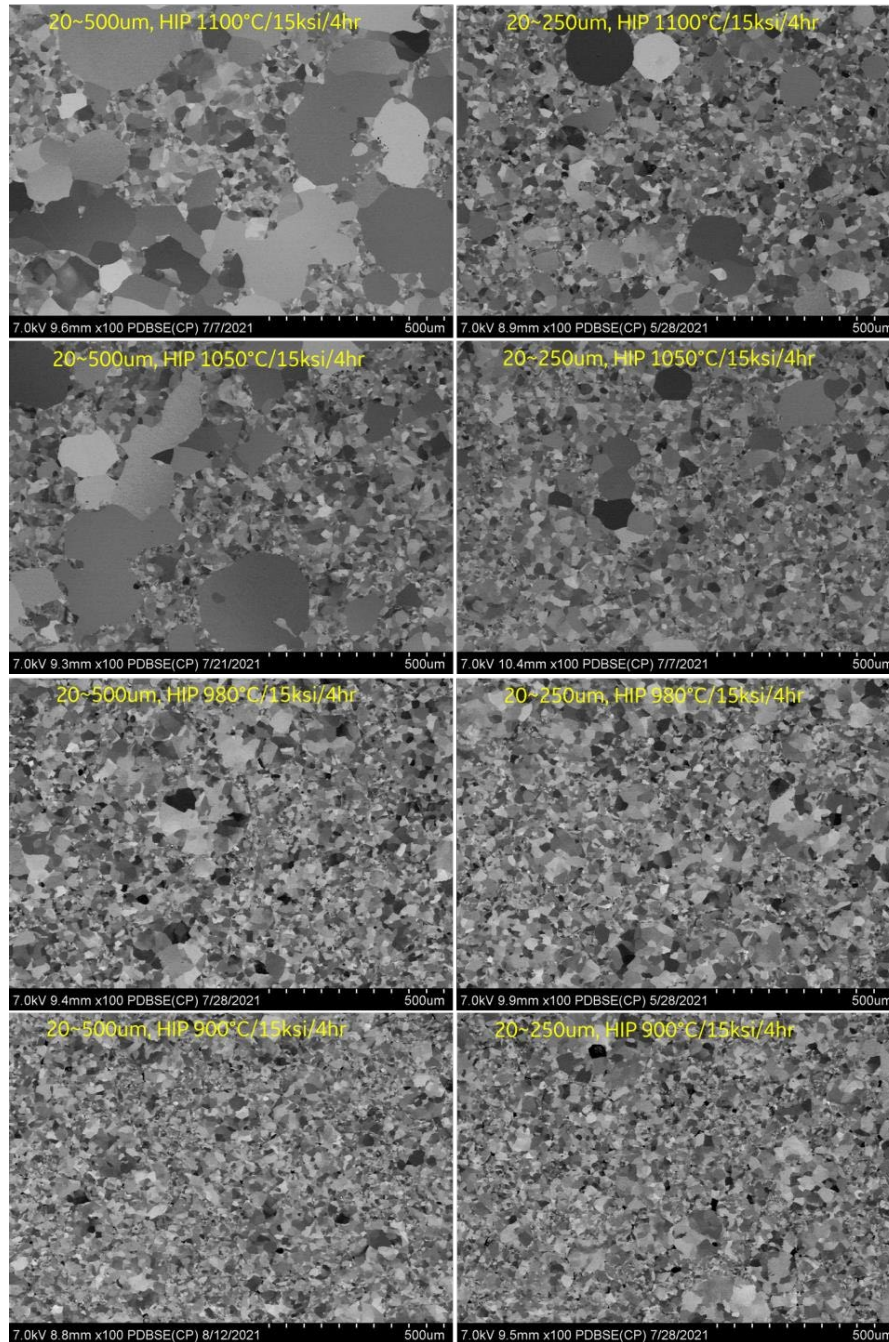


Figure 3: Backscattered electron images of as-HIP grain structures as a function of powder size range and HIP parameters.

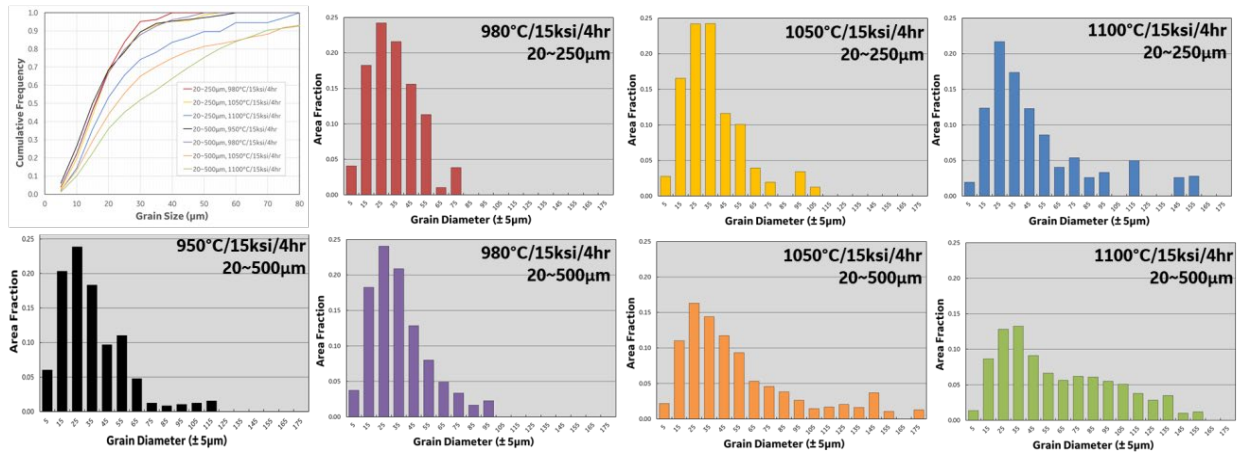


Figure 4: EBSD measured cumulative frequency of grain size and grain size distribution plots for 7 select conditions.

### Influence of Extrusion temperature and Post Annealing

Another PM-C26M powder lot atomized by Oerlikon was used for the subscale HIP and extrusion study. Powder composition (Fe-11.9Cr-6.0Al-1.9Mo) was within the specification range. A narrower powder size range (up to 106  $\mu\text{m}$ ) was used. Three cylindrical HIP cans containing  $\sim 3$  kg powder were HIP'ed at 980°C/25ksi/4hr. The as-HIP grain structure (Fig. 5a) seems much finer possibly caused by finer powder size compared to the coarse powder cut discussed earlier (Fig. 3). After machining to remove the canister material, the three HIP billets were hot extruded at 950, 1000, 1050°C, respectively. Hot extrusion was performed at GE Research on a 1250 Ton Horizontal Loewy Extrusion Press. Starting billet sizes ranged from 3.25" to 3.31" diameter (due to HIPing variation). A nominal 3.5" diameter container was utilized in the press along with a  $\sim 1.13$ " diameter conical die. After extrusion the bars were air cooled to room temperature. Figure 6 shows the as HIP'd powder canisters and the extruded bars (after grit blast).

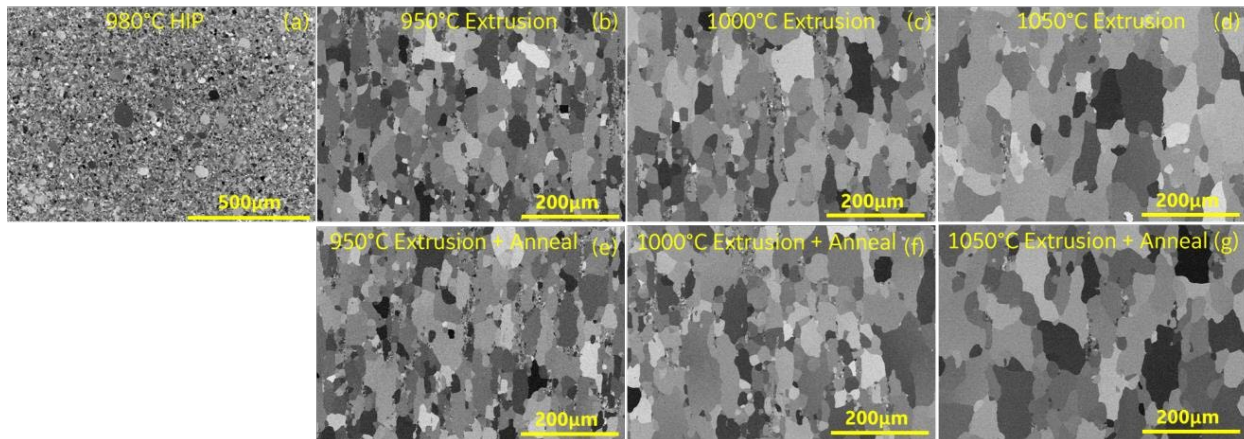


Figure 5: Backscattered electron images of grain structures in (a) the 980°C HIP billets, (b) 950°C extrusion, (c) 1000°C extrusion, (d) 1050°C extrusion; (e) 950°C extrusion followed by 800°C/30min annealing, (f) 1000°C extrusion followed by 800°C/30min annealing, (g) 1050°C extrusion followed by 800°C/30min annealing.

Post extrusion annealing was performed at 800°C for 30 minutes based on prior experience. The as-extruded and post-annealed microstructures are shown in Fig. 5. In general, the extruded microstructure largely shows low retained plastic strain and most grains appeared coarser than asHIP condition. Dynamic recrystallization and grain growth apparently have occurred during the extrusion process. There is still small fraction of fine grain pockets/chains remaining in the

extruded microstructure. The fraction of fine grain pockets decreases with an increase in extrusion temperature from 950°C to 1050°C. The post-annealed grain structures looked similar to the as extruded grain structures, suggesting that 800°C/30min didn't promote further grain growth at the fine grain pockets. The grain size resulting from 950°C extrusion seems adequate for the subsequent tube pilgering process. More detailed future work is required to optimize extrusion conditions, including lower extrusion temperatures, other post anneal conditions, and sensitivity of powder size distribution.



*Figure 6: Three HIP billets and resultant extruded bars produced at different extrusion temperatures.*

### Summary

HIP and extrusion process parameter window was studied for FeCrAl alloy PM-C26M, a candidate material for accident tolerant fuel cladding. Consolidated microstructure proved sensitive to HIP temperature and powder size range, while HIP times of 2 hours vs. 4 hours had little effect. The most reasonable HIP condition that achieved full density and fine grain size was 20 ~ 250  $\mu\text{m}$  powder size range and 980°C/15ksi/4hr HIP condition. HIP temperature below 950°C failed to produce full densified material, while severe grain growth was a concern at HIP temperature above 1050°C particularly for coarse powder range 20 ~ 500  $\mu\text{m}$ . 950°C extrusion yielded reasonable grain structure for the subsequent tube pilgering process. Future work is recommended to optimize extrusion conditions, powder size distribution, mechanical properties of extrusion, and the sensitivity of ductility for the subsequent pilgering process.

### Acknowledgement

This work was funded by US Department of Energy, National Nuclear Security Administration, under award numbers DE-NE0008823 and DE-NE0009047. Sandvik and Oerlikon are acknowledged for producing argon gas atomized C26M powder utilized in this work. American Isostatic Presses is acknowledged for HIP cycle processing.

### References

- [1] K. A. Terrani, Accident tolerant fuel cladding development: Promise, status, and challenges, *Journal of Nuclear Materials*, Vol. 501, (2018) 13-30.  
<https://doi.org/10.1016/j.jnucmat.2017.12.043>
- [2] K. G. Field and S. A. Briggs (2020), "Radiation Effects in FeCrAl Alloys for Nuclear Power Applications," Elsevier Comprehensive Nuclear Materials 2nd edition, Vol. 3.  
<https://doi.org/10.1016/B978-0-12-803581-8.11613-3>
- [3] R. B. Rebak, Accident Tolerant Materials for LWR Fuels, Elsevier, 2020.
- [4] S. Huang, E. Dolley, K. An, D. Yu, C. Crawford, M. A. Othon, I. Spinelli, M. P. Knussman, and R.B. Rebak (2022), "Microstructure and tensile behavior of powder metallurgy FeCrAl accident tolerant fuel cladding," *Journal of Nuclear Materials* 560 (2022) 153524.  
<https://doi.org/10.1016/j.jnucmat.2022.153524>
- [5] R. B. Rebak, T. B. Jurewicz, M. Larsen, L. Yin, Zinc water chemistry reduces dissolution of FeCrAl for nuclear fuel cladding, *Corrosion Science*, Vol. 198 (2022) 110156.  
<https://doi.org/10.1016/j.corsci.2022.110156>